

Measuring the behaviour and properties of carriers in a Silicone probe

Student Number: 199058365

Department of Physics, University of Bath, UK, BA2 7AY
Year 2, Semester 2, [WL]

(Dated: April 30, 2023)

This report aims to investigate the behaviour of carriers in a semiconductor following controlled carrier injection. To achieve this goal, a silicone probe was utilized to evaluate the behaviours of carriers that experienced voltage injections. The properties of this electrical input were modified during the testing process, which allowed for the establishment of experimental relationships between the carriers' behaviours and their causes. Specifically, the study focused on carrier mobility, which was determined to be $103.3 \pm 4.6 \text{ cm}^2/\text{Vs}$, and the diffusion coefficient, which was found to be $2.89 \pm 0.85 \text{ cm}^2/\text{s}$. These results provide insight into how carrier properties and behaviour could showcase macro-properties of the semiconductor, such as temperature or the purity of the doping levels of the probe.

I. INTRODUCTION

In 1948, J.R. Haynes and W. Shockley conducted the Haynes-Shockley experiment [4], which demonstrated that the diffusion of minority carriers in a semiconductor could result in a current. This led to the invention of the point-contact transistor, which revolutionized the field of electronics and enabled the miniaturization of electronic circuits [6]. Today, transistors are present in nearly all electronic devices, including computers, smartphones, and home appliances.

The properties and behaviours of carriers in semiconductors play a vital role in transistor physics. To better understand these properties, this report presents a comprehensive review of carrier properties and recombination effects due to state excitation in a controlled experimental setting. Direct measurements of drift mobility, diffusion coefficient, and recombination lifetimes of excess carriers in semiconductors are compared to existing solid state physics models. The report aims to test the properties of carriers in a semiconductor against predicted values and to add to the existing body of research on this topic.

II. THEORY

Semiconductors are a unique class of materials that exhibit electrical conductivities that are intermediate between those of good conductors and good insulators. This is due to their relatively small energy gap between the filled valence band and the empty conduction band of their electrons [1]. When electrons in semiconductors are excited with sufficient energy, they can move from the valence band to the conduction band, leaving behind a vacancy, commonly referred to as a "hole," in the valence band [2]. This process is illustrated in Figure 1. Holes behave as positive carriers and can move in response to

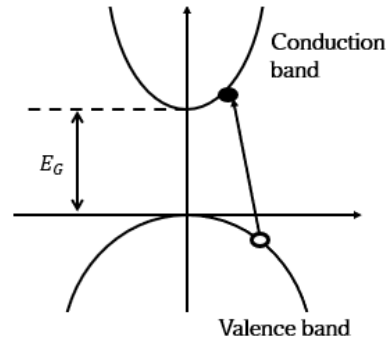


FIG. 1: Theoretical representation of the excitation of an electron from the valence band to the conduction band in a direct band gap semiconductor (does not require a phonon for energy and momentum conservation) and the appearance of a hole in its place.

an applied electric field.

Drude's model provides a theoretical framework for the behaviour of carriers in semiconductors, which assumes that both holes and electrons behave like classical gas particles [7]. This model makes it possible to calculate the velocity of these carriers by using the relationship between the average kinetic energy of a gas molecule and its temperature, which is given by Equation (1).

$$\frac{1}{2}mv_{th}^2 = \frac{3kT}{2} \quad (1)$$

In addition to velocity, carriers have a defined mobility that describes their ease of movement through a material in response to an electric field. This mobility is influenced by factors such as the material's crystal structure, dopant concentration, and temperature. It can be defined as the ratio of the charge of the carrier to its effective mass, multiplied by its relaxation time or scattering time, as given by Equation (2).

$$\mu = \frac{q\tau}{m^*} \quad (2)$$

In this study, the diffusion coefficient of carriers has been a key factor in analyzing carrier diffusion after carrier injection in a semiconductor. Equation (4) defines the diffusion coefficient as the product of the spatial width of the hole pulse in the sample (measured at half peak amplitude) at time t , W , divided by the product of the hole mobility, μ , and the applied voltage, V .

$$t_p = \frac{WL}{\mu V} \quad (3)$$

The spatial width of the hole pulse can be calculated using Equation (5), where D_h is the diffusion constant for holes in n-type material.

$$W = \sqrt{16\ln(2)D_h t} \quad (4)$$

Additionally, Einstein's relationship for a semiconductor (Equation (6)) has been used to study the correlation between the obtained values for diffusion and mobility and the expected semiconductor temperature.

$$T = \frac{Dq}{k\mu} \quad (5)$$

This relationship expresses the temperature, T , as a function of the diffusion constant, D , the charge of the carrier, q , and the carrier mobility, μ , in terms of the Boltzmann constant, k . By using this relationship, the researchers can gain a deeper understanding of how carrier diffusion and mobility are affected by temperature in the semiconductor material being studied.

The relation between carrier mobility and the properties (specifically impurities) of a material was first demonstrated in the 1950 Haynes-Shockley experiment [3], which was partially reproduced as a part of this larger study on semiconductor carriers. The experiment involved measuring the resistance of a thin slice of germanium at different temperatures and doping concentrations. These results showcased an increase of the material's impurities associated with a decrease of the germanium's resistance, indicating an increase in conductivity. The experiment also revealed that the mobility of electrons decreased as the doping concentration increased. Although utilizing a different superconducting material and a different experimental setup from the original experiment, it is important to note that this study builds on this previous discovery and attempts to showcase its proven results in a different setting as well as expand on the study of carrier properties beyond the original experiment's scope.

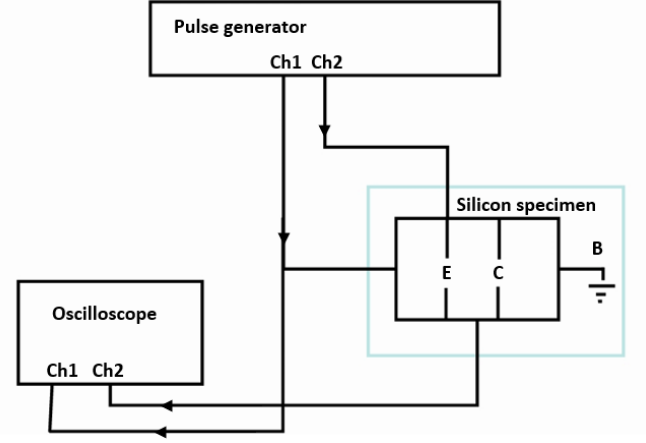


FIG. 2: Schematic diagram of the experimental circuit set-up used. The pulse generator is connected to a silicon specimen which will serve as our superconducting probe through the experiment. An oscilloscope is then attached to the silicon specimen to observe the effects of pulse injections in the material.

III. EXPERIMENTAL

Through most of this experiment, the apparatus was set up as shown in Figure 2. A function generator was set to generate pulse cycles which were delivered to a pure silicon probe. Each pulse had a measured frequency of 1 kHz, with a maximum voltage of 10V and a burst period of 6 μ s. These initial values were set as a starting point for the experiment, and were modified throughout the various tests. These specific starting values were chosen as they were of reasonable magnitude and length.

Through this experiment the drift velocity, mobility, thermal velocity, mean free hole time scatter, carrier diffusion, hole pulse broadening, field reversing and effects of distance when detecting carrier movements were tested. Most of these tests simply required a modification to the initial pulse cycle generation properties, but for the purpose of testing how the distance from the silicon specimen to the collector might affect the results, it is important to understand the architecture of our silicon specimen setup. This setup is illustrated in Figure 3, and showcases a separation of 75 μ m between each of the four collectors and a separation of 225 μ m from our probe to our first collector. The distance between these collectors allows us to better observe the evolution of the carrier injection across the available distance and by distances' relation to time. Unless specified otherwise, all the discussed data in this report was obtained from collector 1.

It is important to note that when outputting a constant field voltage of 6V with our function generator, the obtained voltage using the standard set up was measured at 100 mV. Although this is a considerable loss of voltage through the system, it does correspond with resulting os-

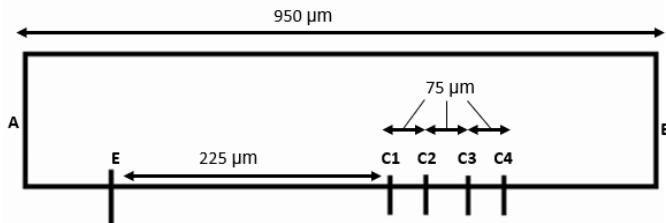


FIG. 3: Schematic diagram of the experimental silicon specimen setup used. To the sides of the set-up the letters A and B showcase the position of the setup with respect to the larger experiment with side B corresponding to the ground connection. As shown in the image, there are 4 available collectors within our setup that are all separated by $75 \mu\text{m}$ between each other, in addition to a $225 \mu\text{m}$ separation from the probe. The complete setup has a length of $950 \mu\text{m}$. In this case, the letter E correspond to the Channel 2 connection from the pulse generator as seen in Figure 2 and thus to the location of our silicon probe.

cilloscope readings and therefore reasonable scaling has been accounted for in the data and figures through this report. This loss is most likely due to noise and attenuation caused by the experimental set-up.

IV. RESULTS AND SPECIFIC DISCUSSION

The presence of carriers in a semiconductor can be observed after a voltage injection into the system. As shown in Figure 4, a short pulse of current is applied to the semiconductor probe, resulting in an observed Gaussian shape in the collected voltage data, and a subsequent negative spike that is equivalent to the original injection. The time of transit of this pulse is measured from the injection spike until the maxima of the Gaussian distribution. This distribution illustrates the rise and decay of excitation of pre-existing carriers in the material. During the first half of the Gaussian, carriers are injected due to pulse excitation. However, after reaching the maxima, this excitation starts to decay until the semiconductor returns to its previous state after the carriers dissipate. This return to its normal state creates an opposite transient voltage, which corresponds to the observed negative spike.

A. Carrier transit time

This subsection examines the transit time of carrier injection through the semiconductor material, which is an important parameter that characterizes how quickly carriers move through the material in response to an applied electric field. The effect of pulse amplitude on the transit time will be presented and illustrated using the

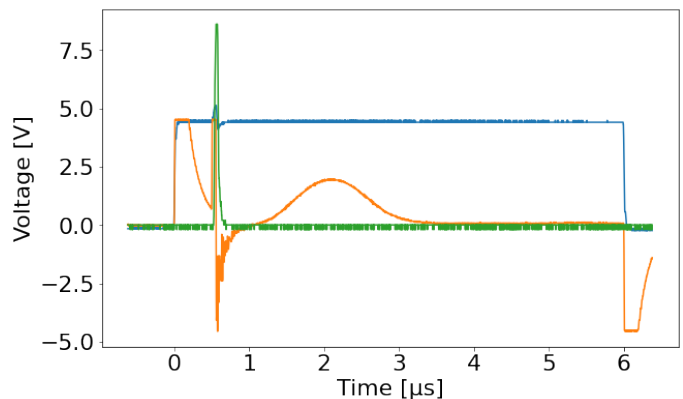


FIG. 4: Voltage output obtained from the standard experimental setup outlined in section II. The green data represents carrier injection, while the orange data displays the voltage collected across the semiconductor. To improve readability, the voltage data has been multiplied by a factor of 10^2 , as described in the experimental section. A Gaussian distribution is observed between 0.5 ns and 3 ns , followed by a negative spike that opposes the injected voltage spike. The blue data shows the field voltage across the setup, which is generally stable, with a small spike during semiconductor voltage injection.

results shown in Figure 5. Additionally, the presence of a Gaussian shape in the obtained results will be discussed in the context of Drude's theory predictions, which suggest that electrons in a conductor act as a classical ideal gas and follow a one-dimensional random walk.

The transit time of the carrier injection through the material was evaluated by comparing the obtained outputs with different pulse amplitudes. Figure 5 illustrates a superposition of the results obtained by these inputs and showcases the "loss" of that Gaussian shape as the voltage of the injected pulse is reduced and thus so are the number of excited carriers.

The Gaussian shape observed in the results is consistent with Drude's theory predictions that electrons in a conductor act as a classical ideal gas that diffuses from high to low concentration, resulting in a Gaussian distribution that can be modeled as a one-dimensional random walk [1]. This argument is supported by the results of two separate random walk simulations shown in Figures 6 and 7, which resulted in a Gaussian shape appearing at the final position with its maxima corresponding to the initial position of the walker.

The drift velocity of carriers in a semiconductor can be determined by evaluating the field voltage against the inverse transit time τ . The carrier transit time is the time it takes for a carrier to move through the semiconductor under the influence of an electric field. The inverse of the transit time is proportional to the carrier mobility μ and the electric field E . This relationship can be expressed by Equation (6):

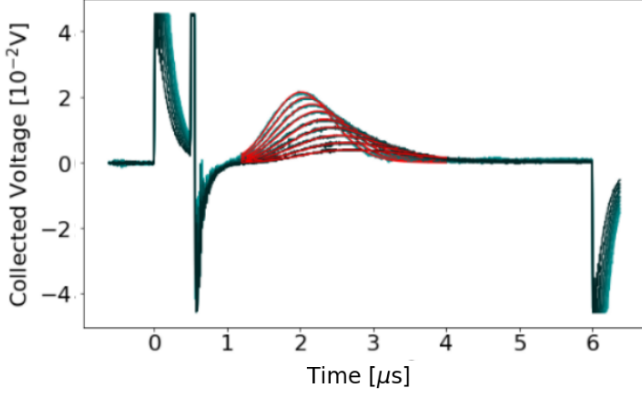


FIG. 5: Collected voltage data using the standard experimental setup, as discussed in the Experimental section, then plotted on a time axis, as observed on an oscilloscope.

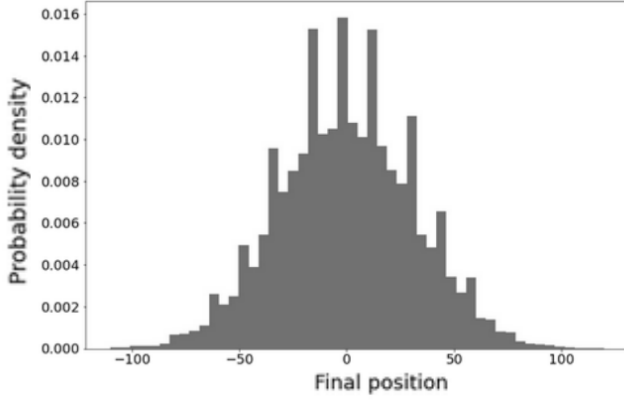


FIG. 6: Results of a simulated 1D quantum walk representing the diffusion of Drude like electrons through a conducting material. The obtained graph showcases a Gaussian distribution when plotting the number of steps taken by the walker (in this case, the electron moving through an arbitrary time unit).

$$v = \mu E = \mu \frac{kT}{q} \frac{1}{\tau} \quad (6)$$

The obtained results for field voltage plotted against the inverse transit time are shown in Figure 8. The graph depicts a linear increase in field voltage with transit time, where the gradient is $2.07 \cdot 10^{-5} \pm 9.12 \cdot 10^{-7}$ and the intercept is -8.03 ± 0.52 .

B. The role of distance

Moving on to evaluate the experimental set-up across collectors at various distances from the probe, as seen in

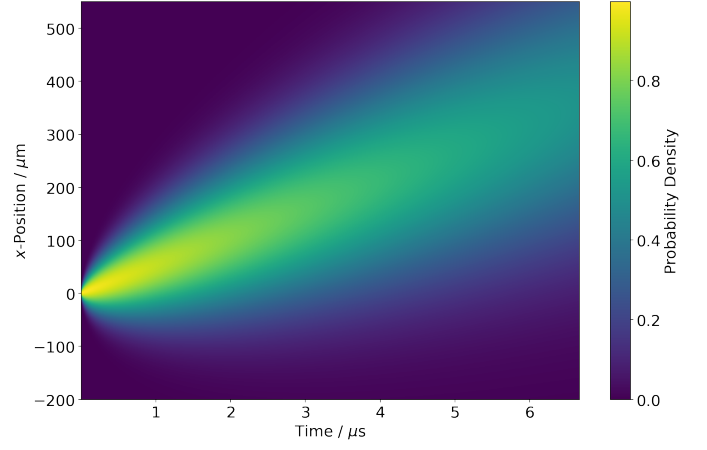


FIG. 7: Results of a simulated 1D quantum walk representing the diffusion of Drude like electrons through a conducting material.

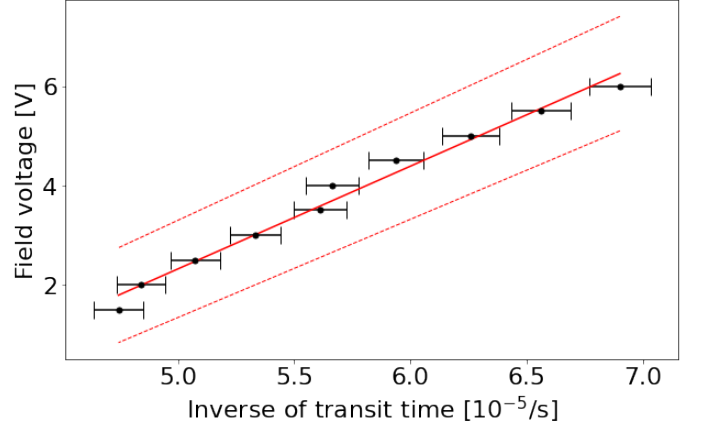


FIG. 8: Field voltage against inverse transit time plotted results. The error bars have been obtained through error propagation through linear regression. The field voltage increases linearly in proportion to transit time, with a gradient of $2.07 \cdot 10^{-5} \pm 9.12 \cdot 10^{-7}$ and an intercept of -8.03 ± 0.52 .

Figure 3, we observe an unexpected skew in the Gaussian shape as the distance from the probe to the capacitor grows. Figure 9 showcases how this loss of the Gaussian shape occurs across the collectors when reading the collected voltage. To provide a more intuitive view of the observed effect, Figure 10 extrapolates the data in a shared distance axis. This allows for a better understanding of how the loss of the Gaussian shape progresses with increasing distance from the probe. The results indicate that the effect is most pronounced at larger distances, with a gradual reduction in the skew as the distance to the probe decreases. It is important to note that the experimental setup has been tested under various conditions and configurations when studying this effect, the results obtained were not influenced by any of the previ-

ously mentioned changes in the standard configuration, such as reasonable voltage input change, or pulse lifetime.

C. The effect of Temperature

Reversing the pulse polarity lead to no voltage drop being collected, as one can observe in Figure 11.

In a similar fashion, Figure 12 demonstrates that the collected voltage across different environmental set-ups overlaps, indicating no significant temperature dependence. This observation aligns with the Drude model, which predicts that the system should not be affected by changes in temperature.

V. GENERAL DISCUSSION

A. Carrier Mobility

As seen in the results section, through experimentation we have observed a correlation between carrier injection input voltage and time duration with carrier mobility. This relation is supported by theory through the following equation:

$$V = \frac{d_3 L}{\mu} \times \frac{1}{t} \quad (7)$$

The relationship allows us to relate our existing data with a linear plot of our systems' received voltage against the inverse of the time measured time, which results in a gradient of $\frac{d_3 L}{\mu}$ that allows us to infer the observed mobility. Using distance $d_3 = 225\mu\text{m}$ and $L = 950\mu\text{m}$, as per Figure 3, we obtain a gradient of linear fit of $2.07 \times 10^{-5} \pm 9.12 \times 10^{-7}$. This gives us a mobility of $\mu = 103.31 \text{ cm}^2/\text{Vs}$. The uncertainty of this mobility is evaluated by:

$$\Delta\mu \approx \left. \frac{d\mu}{dg} \right|_{(g)} \times \Delta g \quad (8)$$

and is equal to $4.57 \text{ cm}^2/\text{Vs}$. Please take note that in Equation 8, the symbol g corresponds to the gradient. Thus giving us a final mobility of $103.31 \pm 4.57 \text{ cm}^2/\text{Vs}$. Our expected mobility should be in the range of 300 to $500 \text{ cm}^2/\text{Vs}$ [5]. These results lead us to suspect the presence of dopants in the probe. Doping refers to the introduction of impurities in a material. Dopants are often defined as intentionally introduced impurities into a material. Given laboratory constraints, we were unable to obtain documentation on our tested probes and therefore cannot confirm on the original purity of these. Nonetheless, regardless of the initial purity of the probes, it is important to know that silicon probes may become less pure over time due to environmental factors such as exposure to moisture, heat, chemical and physical stress, or student misuse of lab equipment. The presence of impurities in utilized samples will have an effect on the predicted mobility ranges.

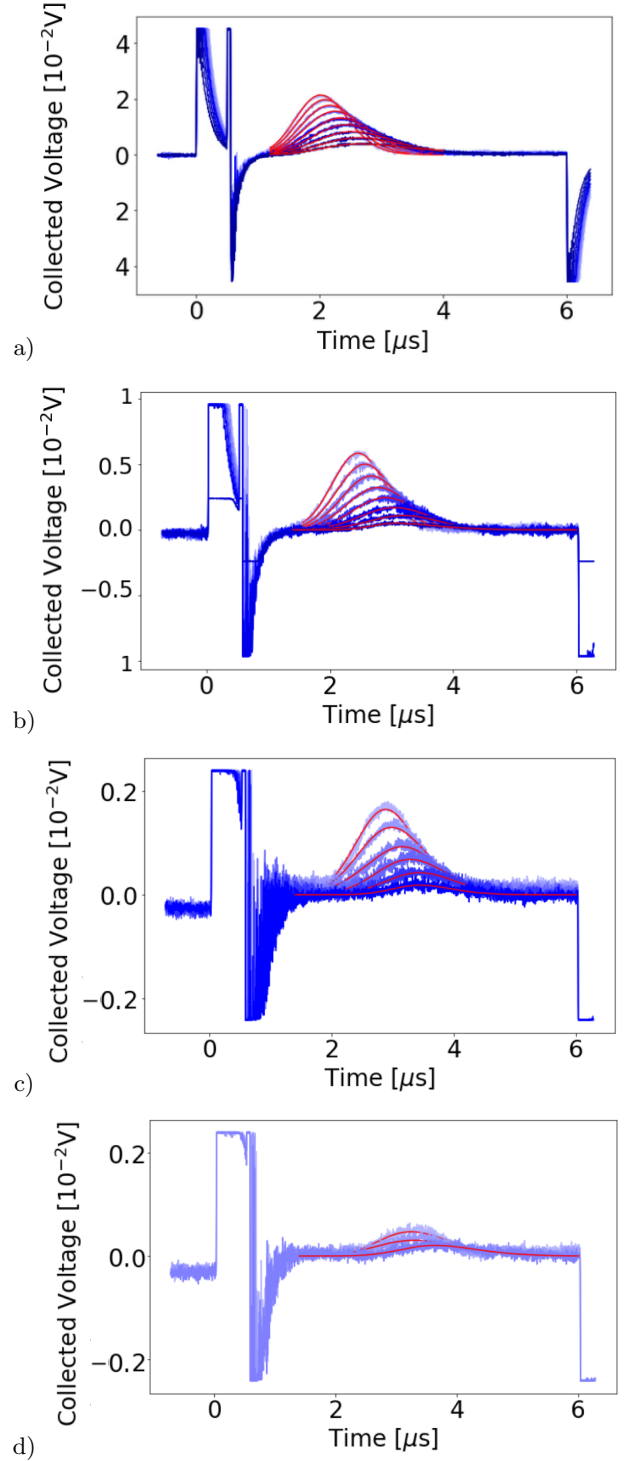


FIG. 9: From left to right, these graphics showcase the obtained collector voltage against time from the closes to the farthest collector from the tested probe. The axis in each of these graphs have been designed to better showcase each individual graph, but are not consistent against each other. One should consider this when comparing the obtained results. As one can observe, the farthest from the probe the capacitor is, the smaller and less Gaussian like the carrier distribution becomes. (a) Collector 1, (b) Collector 2, (c) Collector 3, and (d) Collector 4

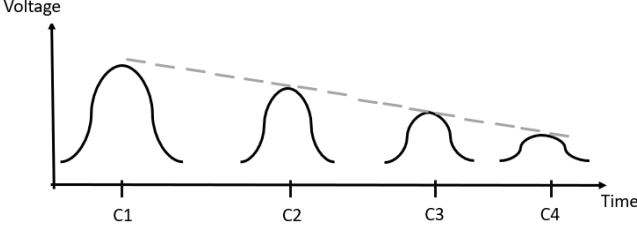


FIG. 10: Graph showcasing the observed evolution of the carrier distribution and decay following the carrier injection across time. As time passes and the signal moves through the four carriers (C1,C2,C3,C4), the Gaussian distribution slowly decreases and loses its shape.

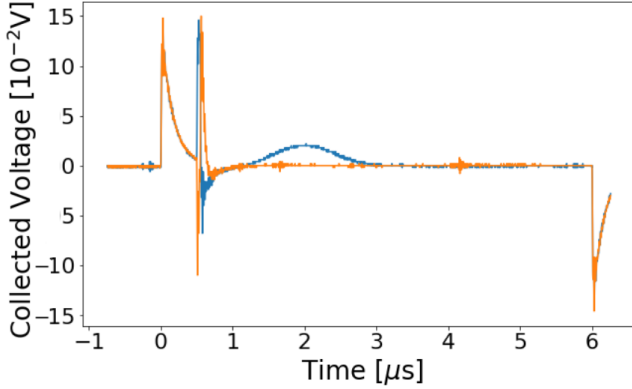


FIG. 11: Pulse reversed polarity showcases no significant change in behaviour in the collected voltage against time results.

B. A Gaussian Diffusion

The consistent presence of a data "skew" across results obtained in all collectors across multiple voltage ranges lead us to believe that the observed skew effect across collectors, discussed in our result section, is caused by the time evolution of the diffusion effects as they occur across the probe. Figure 10 showcases how the diffusion losses of the carrier injection evolve through time and thus become smaller and smaller in the voltage range, which causes a seemed skew of the data across collectors. This effect gives us an insight on the evolution of diffusion across the material. In addition to this observation, we further study the diffusion of carriers through the evaluation of the diffusion coefficient, given by the equation:

$$t_p^2 = t^3 \cdot \frac{16 \ln(2) D_h}{d_3^2} \quad (9)$$

Equation 9 gives us a diffusion coefficient $D_h = 13.27 \pm 1.28 \text{ cm}^2/\text{s}$. The expected diffusion coefficient of pure silicon is approximately $12 \text{ cm}^2/\text{s}$ [5]. In the previous subsection, we observed that the expected mobility of

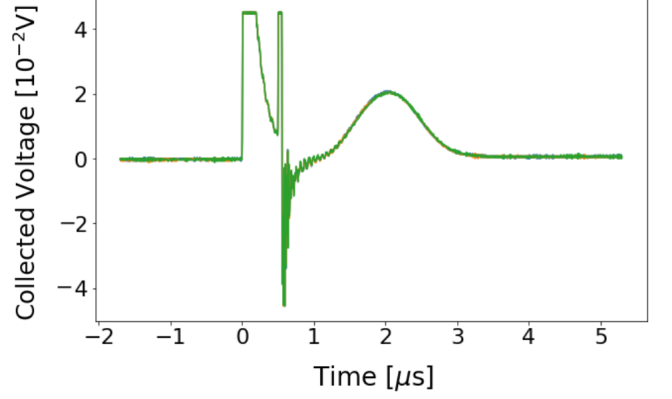


FIG. 12: Collected voltage measured at various environmental temperatures. The data obtained from these measurements show significant overlap, making it challenging to discern between the different lines.

our probe was not consistent with the expected values for pure silicon. As mentioned in the subsection, a natural cause of this could be the use of a doped material. Doped semiconductor diffusion coefficients can decrease up to $2 \text{ cm}^2/\text{s}$. Using data from collector 2 we obtained a diffusion coefficient $D_h = 2.89 \pm 0.85 \text{ cm}^2/\text{s}$. This result seems more consistent with previous evidence, and therefore is the one we utilized for further analysis.

It is important to note that these considerable differences between data across collectors should not be present, regardless of wherever the probe is doped or not. There are many possible causes for these discrepancies, ranging from experimental error to issues with sample preparation or measurement techniques. Therefore, it is important to carefully analyse and control for these factors in future experiments. Further investigation may be necessary to understand the underlying causes of the observed differences in diffusion coefficients and mobility values. This could include more detailed analysis of the material properties and composition, as well as more rigorous testing and calibration of the experimental setup.

Using our diffusion coefficient $D_h = 2.89 \pm 0.85 \text{ cm}^2/\text{s}$, and Einstein's relationship for a semiconductor (Equation 6), we obtain a semiconductor temperature of $T = 324 \pm 95 \text{ K}$, which corresponds to $51.85 \pm 0.95^\circ \text{C}$. Experimentally the expected temperature value would have been of $20 \pm 1^\circ \text{C}$, once again suggesting that the material is behaving differently than expected for a pure silicon sample. This discrepancy in temperature could be attributed to the heat generated by the dopant atoms, which can significantly alter the thermal behaviour of the material.

VI. CONCLUSION

In this experiment, consistent and expected Drude-like carrier behaviour was demonstrated across a silicon

probe. However, the observed errors in the majority of results suggest the presence of impurities in the probes. To confirm the presence of impurities and their effects on the experiment, further investigations should be conducted. Techniques such as X-ray diffraction or energy dispersive spectroscopy could be employed to identify any impurities present and their concentrations. These findings underscore the importance of careful measurement and analysis in the field of semiconductor diffusion and mobility.

VII. MY ROLE ON THE PROJECT

As one of my team's experimentalists, my work on the project focused on obtaining workable data from the experimental set-up and designing tests that were both relevant to our desired project extensions and yielded workable results. In addition to this, through my secondary role as a project manager, I managed the documentation for the team and fulfilled small administrative duties such as setting up and or moving meetings with our project supervisor. As a general team member, I also supported and worked in all other aspects of the project at a smaller

scale.

VIII. REFERENCES

- [1] Ben G. Streetman, Sanjay Kumar Banerjee *Solid State Electronic Devices*, Microelectronics Research Center, University of Texas, 2009
- [2] H.E. Hall *Solid State Physics*, John Willey & Sons Ltd, Mobile electrons, Chapter 3, 1928
- [3] W. Shockley, J.R. Haynes *The Theory of p-n Junctions in Semiconductors and p-n Junction Transistors*, Bell System Technical Journal, 29(4), 569-723, 1950
- [4] J. R. Haynes, W. Shockley *Investigation of Hole Injection in Transistor Action*, Bell Telephone Laboratories, Phys. Rev. 75, 691, 1948
- [5] M. B. Prince *Drift Mobilities in Semiconductors. II. Silicon*, Phys. Rev. 93, 1204, 1954
- [6] W. A. Atherton *Miniaturization of Electronics*, From Compass to Computer: A History of Electrical and Electronics Engineering, 237-267, Macmillan Education UK, London, 1984
- [7] J Singleton *Band theory and electronic properties of solids*, Metals: The Drude and Sommerfeld Models, Chapter 1, Oxford University Press, London, 2001